Int. J. Electrochem. Sci., 6 **(2011)** 1027 - 1044

International Journal of ELECTROCHEMICAL SCIENCE
www.electrochemsci.org

Experimental and Quantum Chemical Studies on the Corrosion Inhibition Potentials of 2-(2-Oxoindolin-3-Ylideneamino) Acetic Acid and Indoline-2,3-Dione

Nnabuk O. Eddy [1,*], *Benedict I. Ita* [2], *Nkechi E. Ibisi* [3], *Eno E. Ebenso* [4,*]

[1] Department of Chemistry, Ahmadu Bello University, Zaria, Nigeria.
[2] Department of Chemistry, University of Calabar, Calabar, Nigeria.
[3] Department of Chemistry, Michael Okpara University of Agriculture, Umudike, P. M. B. 7267, Umuahia, Nigeria.
[4] Department of Chemistry, North West University (Mafikeng Campus), Private Bag X2046, Mmabatho 2735, South Africa.
[*]E-mails: nabukeddy@yahoo.com, Eno.Ebenso@nwu.ac.za

Received: 15 February 2011 / *Accepted:* 8 March 2011 / *Published:* 1 April 2011

The inhibition potentials of 2-(2-oxoindolin-3-ylideneamino) acetic acid (IG) and Indoline-2,3-dione (IS) was carried out using gravimetric and gasometric methods while the theoretical approach was investigated using quantum chemical principles. The results obtained, indicated that IG and IS inhibited the corrosion of mild steel in HCl solution through the mechanism of chemical adsorption. The adsorption of the inhibitors is spontaneous, endothermic and is consistent with El Awardy et al kinetic model. Application of Dubinin-Radushkevich adsorption isotherm also ascertained the prevalence of chemisorption mechanism. The Fukui function, global softness and Huckel charges on carbon and electronegative elements in IG and IS revealed that the site for electrophilic attack is in the pyrrole nitrogen while the site for nucleophilic attack is in the phenyl ring. It was also found that the inhibition potential of IG is better than that of IS because the presence of methylenecarbamic acid group in IG (=NCH_2CO_2H) facilitated better adsorption than the =O group in IS.

Keywords: Corrosion inhibition, 1H indole derivatives, experimental and quantum studies

1. INTRODUCTION

In the oil, fertilizer, metallurgical and other industries, valuable metals (such as mild steel, aluminium and zinc) are prone to corrosion when they come in contact with aggressive medium during acid cleaning, pickling, etching and other related industrial processes [1-5]. In order to fight against

this environmental consequence, several approaches have been designed to protect metallic installations in industries. However, one of the most effective and preferred option involves the use of inhibitors [6-11].

A careful examination of literature reveals that most corrosion inhibitors are organic compounds that have hetero atoms and functional groups that are capable of facilitating the adsorption of the inhibitor onto the metal surface [12]. The adsorption of the inhibitor onto the metal surface proceeds through charge transfer from the charged inhibitor's molecule to the charged metal (physical adsorption) or by electron transfer from the inhibitor' molecule to the metal (chemical adsorption). In all cases, chemisorption succeeds physiosorption; therefore, corrosion inhibition process can be viewed as a process that involves electrophilic and nucleophilic attack [13].

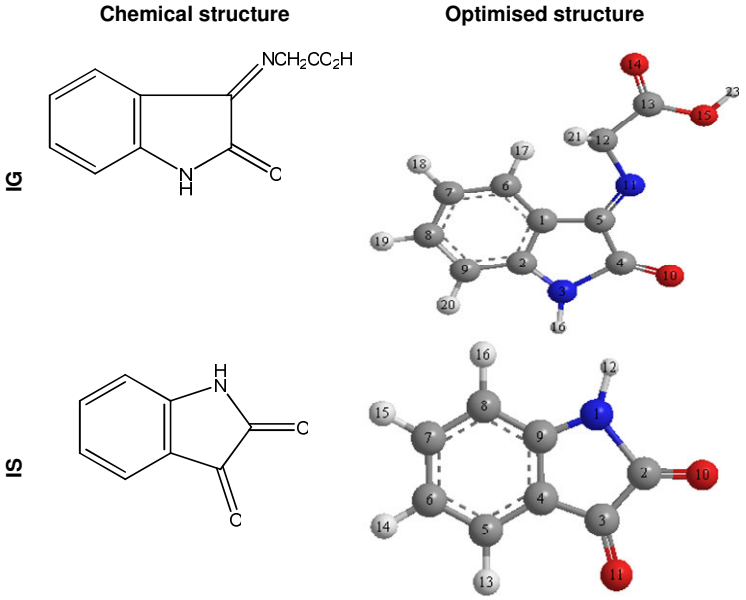

Figure 1. Chemical and optimised structures of IG and IS

In spite of the broad spectrum of inhibitors chosen from organic compounds, it is significant to note that the search for corrosion inhibitors that have optimum efficiency is still going on. Literature is also scanty on the use of indoline or its derivatives as corrosion inhibitors. Therefore, the present study is aimed at investigating the corrosion inhibition potentials of 2-(2-oxoindolin-3-ylideneamino) acetic acid (IG) and indoline-2,3-dione (IS). The chemical and optimised structures of IG and IS are shown in Fig. 1. From Fig. 1, it can be seen that IG and IS are aromatic compounds that have hetero atom (N) in the pyrrole ring, in addition to =O bond. Hence, IG and IS are expected to be good inhibitors for the corrosion of mild steel.

Gravimetric and gasometric methods were used to investigate the inhibition potentials of IG and IS and the results obtained from both compounds were compared with each other using semi-empirical data. From global and local selectivity indices, the sites for electrophilic and nucleophilic

attacks in IG and IS were investigated in order to give more evidence to the elucidation of the mechanism of inhibition.

2. EXPERIMENTAL TECHNIQUES

2.1. Materials

Materials used for the study were mild steel sheet of composition (wt %); Mn (0.6), P (0.36), C (0.15) and Si (0.03) and the rest Fe. The sheet was polished and mechanically pressed cut into different coupons, each of dimension, 5x4x0.11cm. Each coupon was degreased by washing with ethanol, dipped in acetone and allowed to dry in the air before they were preserved in a desicator. All reagents used for the study were Analar grades and double distilled water was used for their preparation.

The concentrations of the inhibitors were within the range, 1 x 10^{-4} to 5 x 10^{-4} M. Each of these concentrations were used to prepare different test solutions by dissolving them in 0.1 M HCl (for use in gravimetric analysis) and in 2.5 M HCl (for use in gasometric analysis) respectively.

2.2. Gravimetric method

In the gravimetric experiment, a previously weighed metal (mild steel) coupon was completely immersed in 250 ml of the test solution in an open beaker. The beaker was covered with aluminium foil and was inserted into a water bath maintained at 303 K. After every 24 hours, the corrosion product was removed by washing each coupon (withdrawn from the test solution) in a solution containing 50 % NaOH and 100 g l^{-1} of zinc dust. The washed coupon was rinsed in acetone and dried in the air before re-weighing. The experiment was also repeated at 313, 323 and 333 K. In each case, the difference in weight for a period of 168 h was taken as the total weight loss. From the average weight loss results (average of three replicate analysis), the inhibition efficiency (%I) of the inhibitor, the corrosion rate of mild steel and the degree of surface coverage were calculated using equations 1, 2 and 3 respectively [14,15] ;

$$\%I = (1 - W_1/W_2) \times 100 \quad (1)$$

$$CR = (W_2 - W_1)/At \quad (2)$$

$$\theta = 1 - W_1/W_2 \quad (3)$$

where W_1 and W_2 are the weight losses (g) for mild steel in the presence and absence of the inhibitor respectively, CR is the corrosion rate of mild steel in $gcm^{-2}h^{-1}$, A is the area of the mild steel (in cm^2), t is the total period of immersion (in hours) and θ is the degree of surface coverage of the inhibitor.

2.3. Gasometric method

Gasometric methods were carried out at 303 K using a gasometer. In each case, the metal coupon was inserted into the round bottom flask (containing the test solution) of the gasometer. The volumes of hydrogen gas evolved were measured after every minute until a steady value was obtained. From the volume of hydrogen gas evolved per minute, inhibition efficiencies were calculated using equation 4 [16].

$$\%\mathrm{I} = \left(1 - \frac{V_{Ht}^{1}}{V_{Ht}^{o}}\right) x\,100 \qquad 4$$

where V_{Ht}^{1} and V_{Ht}^{o} are the volumes of H_2 gas evolved at time, 't' for inhibited and uninhibited solutions respectively.

2.4. Computational techniques

Single point energy calculations were carried out using AM1, PM6, PM3, MNDO and RM1 Hamiltonian in the MOPAC 2008 software for Windows [17]. Calculations were performed on an HP Pentium V (2.0 GHz, 4 GB RAM and 250 GB hard disc) computer. The quantum chemical indices calculated were, the energy of the highest occupied molecular orbital (E_{HOMO}), the energy of the lowest unoccupied molecular orbital (E_{LUMO}), the dipole moment (μ), and the total energy (TE). The Muliken and Lowdin charges (q) for nucleophilic and electrophilic attacks were computed using GAMESS computational software [18]. Correlation type and method used for the calculation was DFT while the basis sets was fixed at 6-13G.

3. RESULTS AND DISCUSSION

3.1. Effect of IG and IS

Table 1 shows values of inhibition efficiencies of various concentrations of IG and IS for the corrosion of mild steel in 0.1 M HCl. It can be seen that the inhibition efficiencies of IG and IS increase with increasing concentration and with increase in temperature. Therefore, IG and IS are adsorption inhibitors and their adsorption supports the mechanism of chemical adsorption. For an adsorption inhibitor, the inhibition efficiency is expected to increase with increase in concentration [19]. Also, the mechanism of chemical adsorption is characterized by increasing value of inhibition efficiency as the temperature is increased [20].

Values of inhibition efficiency obtained from gasometric measurements are also presented in Table 1. The results obtained, indicate that the inhibition efficiencies obtained from hydrogen evolution measurements are higher than those obtained from gravimetric method.

Table 1. Inhibition efficiencies of IG and IS for the corrosion of mild steel in HCl solutions

System	Gravimetric				Gasometric
	303 K	313 K	323 K	333 K	303 K
1 x10^{-4} M IG	48.01	54.00	65.11	72.32	54.67
2 x 10^{-4} M IG	50.12	58.04	68.13	75.33	64.46
3 x 10^{-4} M IG	54.23	62.02	70.02	80.22	72.33
4 x 10^{-4} M IG	58.22	65.03	74.00	81.04	74.24
5 x 10^{-4} M IG	60.21	72.01	79.02	87.07	78.33
1 x10^{-4} M IS	10.01	15.23	38.28	45.04	36.87
2 x 10^{-4} M IS	12.02	18.54	40.07	50.23	41.23
3 x 10^{-4} M IS	15.07	20.08	48.00	58.23	45.34
4 x 10^{-4} M IS	18.34	30.09	50.34	60.24	52.34
5 x 10^{-4} M IS	19.09	38.34	55.19	84.04	54.21

This implies that the instantaneous inhibition efficiencies (obtained from gasometric measurements) of IG and IS are better than their average inhibition efficiency (obtained from gravimetric measurements). However, values of inhibition efficiency obtained from the two analytical methods correlated strongly (R^2 = 0.9931 and 0.9207 for IG and IS respectively).

3.2. Effect of temperature

The activation energies for the inhibition of the corrosion of mild steel by IG and IS were calculated using the Arrhenius equation [21].

$$CR = A \exp(-E_a/RT) \quad (5)$$

where CR is the corrosion rate of mild steel, A is the Arrhenius or pre-exponential factor, E_a is the activation energy, R is the molar gas constant and T is the temperature. Transformation of equation 5, using logarithm function, yields equation 6

$$\log CR = \log A - E_a/2.303RT \quad (6)$$

From equation 6, a plot of logCR versus 1/T should be linear with slope and intercept equal to E_a/2.303 and logA respectively. Fig. 2 shows the Arrhenius plots for the corrosion of mild steel in solutions of HCl, containing various concentrations of IG and IS. Values of the activation energy, the degree of linearity (R^2) and the pre-exponential factor deduced from the Arrhenius plots are presented in Table 2. From the results obtained, the activation energies for the inhibited systems ranged from 24.31 to 160.19 kJ/mol and from 28.03 to 135.75 kJ/mol for IG and IS respectively. These values are higher than the value obtained for the blank solution indicating that the corrosion reaction of mild steel in HCl solution is retarded by various concentrations of IG and IS. The calculated results also indicate that the mechanism of chemical adsorption exceeded physical adsorption.

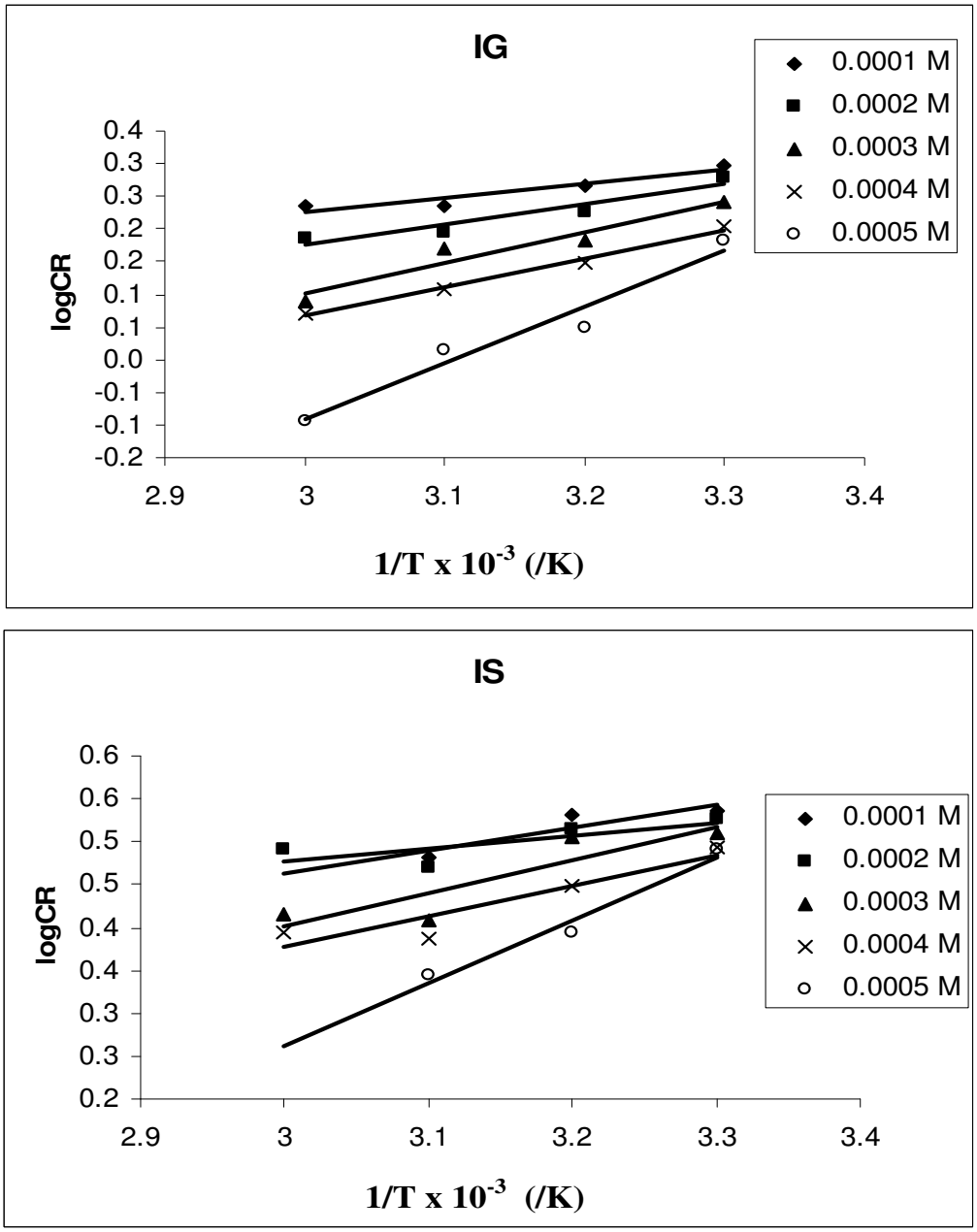

Figure 2. Variation of log CR with 1/T (Arrhenius plots) for the inhibition of the corrosion of mild steel at various concentrations of IG and IS.

3.3. Thermodynamic and adsorption studies

In order to calculate thermodynamic parameters for the adsorption of IG and IS on mild steel surface, the transition state equation (equation 7) was used;

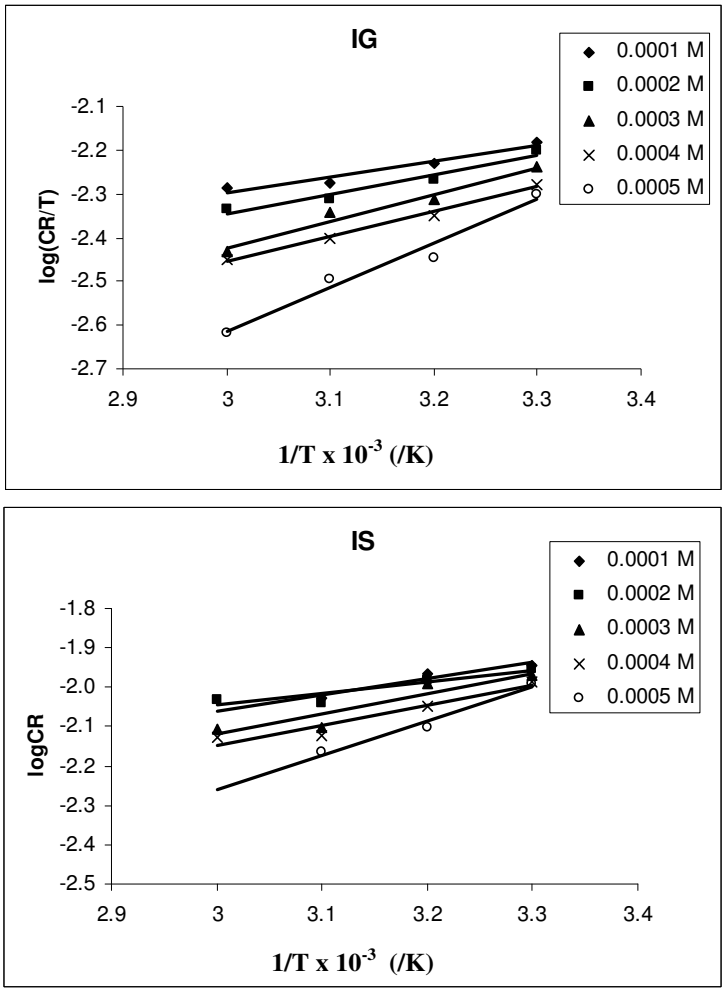

Figure 3. Variation of log (CR/T) with 1/T (Transition state plots) for the inhibition of the corrosion of mild steel at various concentrations of IG and IS.

Table 2. Kinetic and thermodynamic parameters for the adsorption of IS and IG on mild steel surface.

System	E_a (kJ/mol)	A	R^2	ΔH_{ads} (kJ/mol)	ΔS_{ads} (kJ/mol)	ΔG^0_{ads} (kJ/mol)	R^{2**}
Blank	24.31	19.21	0.9765	3.42	-165.32		
1 x10^{-4} M IG	40.21	0.65	0.8778	6.78	-133.29	-40.38	0.9481
2 x 10^{-4} M IG	57.86	0.47	0.9076	8.60	-126.83	-38.42	0.9513
3 x 10^{-4} M IG	80.33	0.29	0.9879	11.65	-116.27	-35.22	0.9638
4 x 10^{-4} M IG	87.30	0.27	0.9405	10.93	-117.79	-35.68	0.9924
5 x 10^{-4} M IG	160.19	0.07	0.9606	19.19	-89.96	-27.24	0.9701
1 x10^{-4} M IS	49.83	1.41	0.8172	7.81	-134.71	-40.81	0.9129
2 x 10^{-4} M IS	28.03	1.02	0.7022	5.52	-141.88	-42.99	0.8431
3 x 10^{-4} M IS	71.65	2.14	0.7913	10.03	-126.90	-38.44	0.8738
4 x 10^{-4} M IS	67.02	2.03	0.8708	9.55	-127.85	-38.73	0.9259
5 x 10^{-4} M IS	135.75	6.95	0.9668	16.70	-104.19	-31.55	0.9758

R^2 = degree of linearity for Arrhenius plot and R^{2**} = degree of linearity for the transition state plot

$$CR = (RT/Nh)\exp(\Delta S_{ads}/R)\exp(-\Delta H_{ads}/RT) \quad 7$$

where CR is the corrosion rate of mild steel, h is the Planck constant, R is the molar gas constant, N is the Avogadro's number, ΔS_{ads} is the entropy of adsorption and ΔH_{ads} is the enthalpy of adsorption [22]. Taking the logarithm of both sides of equation 7 yields equation 8,

$$\log(CR/T) = \log(R/Nh) + \Delta S_{ads}/2.303R - \Delta H_{ads}/2.303RT \quad 8$$

From equation 8, the plots of log(CR/T) versus 1/T should yield a straight line with slope equal to $-\Delta H_{ads}/R$ and intercept equal to $(\log(R/Nh) + \Delta S_{ads}/R)$. Fig. 3 shows the transition state plots for inhibited corrosion reaction of mild steel. Calculated values of R^2, ΔS_{ads} and ΔH_{ads} are presented in Table 2. From the results obtained, it is evident that the corrosion data obeyed the assumptions establishing the transition state theory. Calculated values of ΔH_{ads} were positive indicating that the adsorption of IG and IS on mild steel surface is endothermic. On the other hand, values of ΔS_{ads} deduced from the intercept of the plots were negative which also indicate that the adsorption of IG and IS on mild steel surface occurred with increasing degree of orderliness. It was also found that values of pre-exponential factor deduced from the Arrhenius plots (Fig. 2) correlated strongly with those of ΔS_{ads} as indicated in Fig. 4. Correlation between ΔH_{ads} and E_a was also good ($R^2 = 0.8356$).

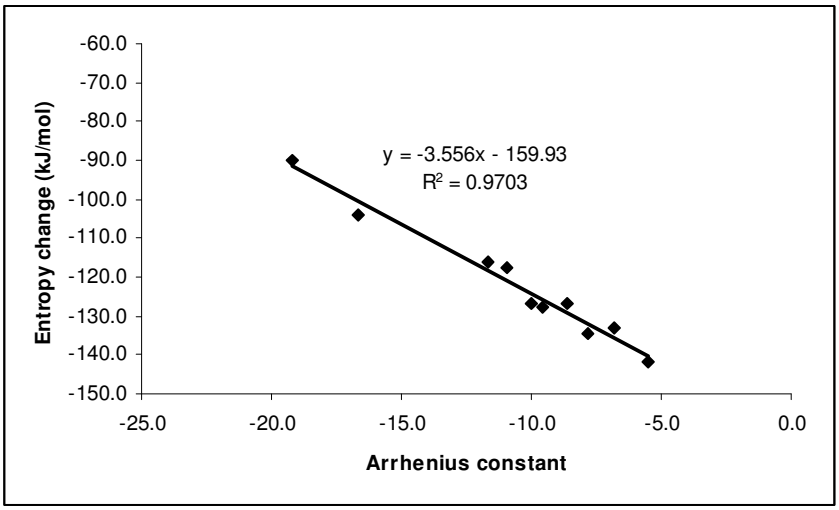

Figure 4. Variation of entropy of adsorption of IG and IS with the Arrhenius constant**.**

This can be explained as follows. If we equate the right hand side of the Arrhenius equation (equation 6) with that of the transition state equation (equation 8), it can be seen that the pre-exponential factor (A) is related to ΔS_{ads} while the activation energy is related to ΔH_{ads}. Quantitative treatments rendered on some corrosion reactions by Mohana and Badiea [23] has shown that the relation between ΔH_{ads} and E_a is $\Delta H_{ads} = E_a - RT$.

We also calculated the standard free energy of adsorption of IG and IS by substituting calculated values of ΔH_{ads} and ΔS_{ads} into the Gibb Helmholtz equation, which can be written as follows,

$$\Delta G^0_{ads} = \Delta H_{ads} - T\Delta S_{ads} \quad 9$$

Calculated values of ΔG^0_{ads} are also recorded in Table 2. The results obtained, indicate that the free energies are negative and are within the range of values expected for the mechanism of chemical adsorption. Therefore, the adsorption of IG and IS on mild steel surface is spontaneous and is consistent with the transfer of electron from the inhibitor's molecule to Fe^{2+} in mild steel, which indicate chemisorption.

Table 3. El awardy et al and Dubinin-Radushkevich adsorption parameters for the inhibition of the corrosion of mild steel in HCl by IG and IS

System	logK'	logK	y	x	ΔG^0_{ads} (kJ/mol)	R^2	E_{ads} (kJ/mol)
IG at 303 K	1.0127	2.0372	0.4971	2.0117	-21.91	0.9631	7.91
IG at 313 K	2.0811	2.8764	0.7235	1.3822	-27.67	0.8218	7.83
IG at 323 K	1.4760	3.4350	0.4297	2.3272	-32.00	0.9006	8.56
IG at 333 K	1.7600	3.7849	0.4650	2.1505	-35.23	0.9571	8.73
IS AT 303 K	1.2073	3.8145	0.3165	3.1596	-32.23	0.9223	7.70
IS at 313 K	1.8003	4.0851	0.4407	2.2691	-34.91	0.8754	7.56
IS at 323 K	1.8077	4.6021	0.3928	2.5458	-39.22	0.8327	8.46
IS at 333 K	2.4777	4.7140	0.5256	1.9026	-41.15	0.8447	8.12

The adsorption characteristics of IG and IS was investigated by fitting data obtained from weight loss measurements into different adsorption isotherms. The test revealed that the adsorption of IG and IS on mild steel surface can best be described by Dubinin-Radushkevich and by El Awardy *et al* (kinetic model) adsorption models. The kinetic-thermodynamic model can be expressed as follows [24],

$$\log(\theta/(1-\theta)) = \log K' + y\log C \quad 10$$

where K' is a constant and is related to the binding constant, K as follows,

$$K = K'^{(1/y)} \quad 11$$

where y is the number of the inhibitor molecules occupying one active site and 1/y = x is the number of active sites of the surface occupied by one molecule of the inhibitor. It has been found that values of x greater than unity indicates that a given inhibitor molecule will occupy more than one

active site. Large values of the binding constant mean better inhibition efficiency of a given compound (i.e. stronger electrical interaction for the adsorbing molecules at the surface of the metal). Small values of the binding constant, however, indicate that such interaction by the adsorbing molecules and the metal surface are weaker, denoting that the molecules are easily removed by the solvent molecules from the surface.

Fig. 5 shows El Awardy et al kinetic-thermodynamic isotherm for the adsorption of IG and IS on mild steel surface. Adsorption parameters deduced from the plots are presented in Table 3. From the results obtained, it is evident that the degree of linearity for the isotherms ranged from 0.8327 to 0.9631, indicating that the adsorption of IG and IS supports the kinetic-thermodynamic model. Values of x were approximately equal ($x \approx 2$) for all concentrations of IS and IG. Therefore the adsorption of IS and IG on mild steel surface can be regarded as a substitution process, in which an inhibitor molecule (In_{inh}) in the aqueous phase substitutes an x (in this case, x = 2) number of water molecules adsorbed on the surface as shown in the equation below,

$$Inh_{(sc\,n)} + 2H_2O \rightleftharpoons Inh_{(acs)} + 2H_2O_{(sc\,n)} \qquad 12$$

The above step may be preceded by the inhibitor's molecules combining with Fe^{2+} ions (in mild steel) on the metal surface to form metal-inhibitor complex. The resulting complex could either inhibit or catalyze further metal dissolution depending on its solubility.

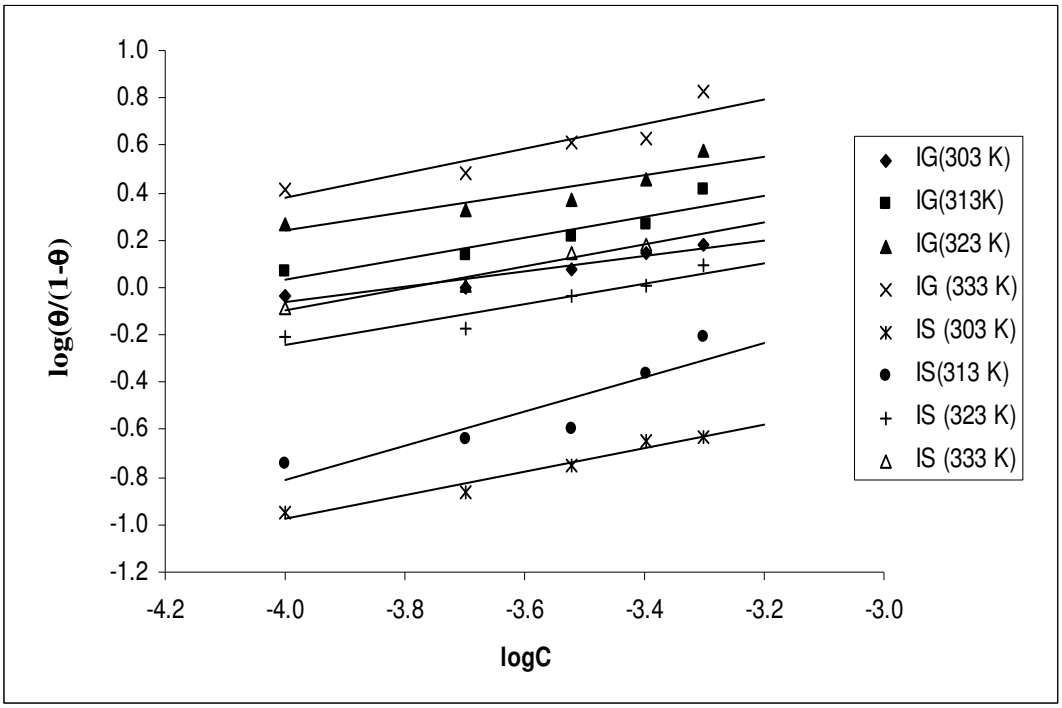

Figure 5. El Awardy et al isotherm for the adsorption of IS and IG on mild steel surface at various temperatures.

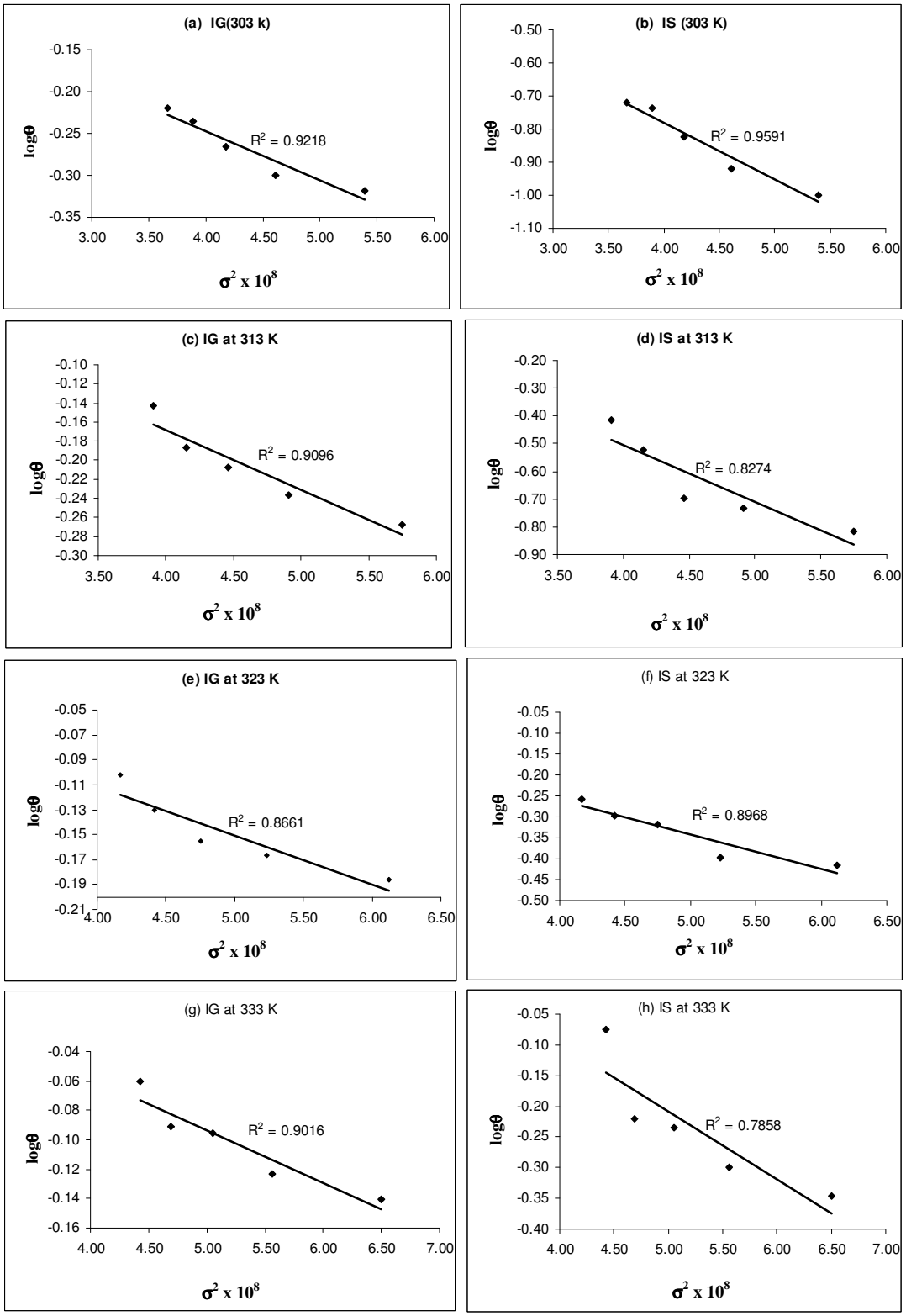

Figure 6. Dubinin-Radushkevich isotherm for the adsorption of IG and IS on mild steel surface at various temperatures.

An iron anodic oxidation mechanism, which is valid in the presence of the inhibitor, could be similar to that discussed by Mc Cafferty and Hackerman and also by Sternberg and Branzoi [25].

Fe	+ H_2	=	$Fe.H_2O_{ads}$			13
$Fe.H_2O$	+ Inh	=	$FeOH^-$	+	H_2O	14
$Fe.H_{2ads}$	+ Inh	=	$FeInh_{ads}$	+	H_2O	15
$FeOH^-_{ads}$		=	$FeOH_{ads}$	+	e^-	16
$FeInh_{ads}$		=	$FeInh^+_{ads}$	+	e	17
$FeOH_{ads}$	+ $FeInh^+$	=	$FeInh_{ads}$	+	$FeOH^-$	18
$FeOH^+$	+ H^+	=	Fe^{2+}	+	H_2O	19

where Inh are the inhibitor molecule. The above mechanism indicate that the anodic reaction kinetics is affected by two intermediates: one involving adsorbed hydroxyl ($FeOH_{ads}$) and the other involving the adsorbed inhibitor molecule ($FeInh_{ads}$). The rate of anodic dissolution (step 4: equation 16) depends on the product of step 2 (equation 14) but two competitive steps (2 and 3: equations 14 and 15) are based on the $Fe.H_2O_{ads}$. Displacement of the adsorbed water molecule by the specie Inh can affect step 4 (equation16).

Every condition, such as molecular shape or localised partial charges or by another view, strict hindrance of Inh molecule to the metal surface, can variegate the above competition. The influence of two solvents on each inhibitor molecules causes dispersion of the inhibition ability. This dispersion may accelerate the adsorption of the inhibitor molecule onto the different metal surfaces sites having different activation energies for chemisorptions (lattice planes, edges, dislocation, in homogeneities, etc).

Dubinin-Radushkevich adsorption isotherm can be used to distinguish between physical and chemical adsorption and can be expressed as follows [26] .

$$\ln\theta = \ln\theta_{max} - a\sigma^2 \qquad 20$$

where θ_{max} is the maximum surface coverage and σ (Polany potential) can be written as

$$\sigma = RT\ln(1 + 1/C_{inh}) \qquad 21$$

The constant, σ gives the mean adsorption energy, E_{ads} which is the transfer energy of 1 mole of adsorbate from infinity (bulk solution) to the surface of the adsorbent

$$E_{ads} = 1/(2a)^{1/2} \qquad 22$$

The magnitude of E gives information about the type of adsorption. If this value is less than or equal to 8 kJ/mol, adsorption type can be explained by physical adsorption. Fig. 6 shows the Dubinin-Radushkevich isotherm for the adsorption of IG and IS on mild steel surface. Values of R^2 (indicated in the plots) obtained from the plots reveals that Dubinin-Radushkevich isotherm is applicable to the

adsorption of IG and IS on mild steel surface. Values of the adsorption energy (E_{ads}) deduced from the plots are recorded in Table 3. From the results obtained, it can be seen that the adsorption energies signified the ascent of chemisorption after physiosorption.

The equilibrium constant of adsorption calculated from the intercept of the El Awardy kinetic model is also related to the standard free energy of adsorption of the inhibitors as follows,

$$\Delta G^{0}_{ads} = -2.303RT\log(55.5K) \qquad 23$$

where R is the gas constant, T is the temperature and 55.5 is the concentration of water at electrode/electrolyte interface in mol/L [27]. Values of ΔG^{0}_{ads} computed from equation 23 are recorded in Table 3. Calculated values of the free energy are also negative and are comparable to those obtained from the Gibb Helmholtz equation.

3.4. Quantum chemical study

Table 4 shows some quantum chemical parameters calculated for IG and IS using PM6, PM3, AM1, RM1 and MNDO Hamiltonians.

Table 4. Quantum chemical parameters for the studied inhibitors

	Models	E_{HOMO} (eV)	E_{LUMO} (eV)	ΔE (eV)	E_N (eV)	E_{N-1} (eV)	E_{N+1} (eV)	IE (eV)	EA (eV)	S (eV^{-1})	η (eV)	χ (eV)
IG	PM6	-9.283	-2.067	7.216	-1805.24	-1796.70	-1807.89	8.54	2.65	0.17	5.88	5.60
	PM3	-8.887	-1.486	7.401	-1770.06	-1761.79	-1772.05	8.27	1.99	0.16	6.25	5.13
	AMI	-9.007	-1.450	7.557	-1935.19	-1926.88	-1937.21	8.31	2.02	0.16	6.25	5.17
	RMI	-8.916	-1.301	7.615	-1911.02	-1902.83	-1912.90	8.19	1.88	0.16	6.25	5.04
	MNDO	-8.984	-1.375	7.609	-1939.52	-1931.24	-1941.49	8.28	1.97	0.16	6.25	5.13
IS	PM6	-9.127	-1.603	7.524	-2561.66	-2553.32	-2564.02	8.34	2.36	0.17	5.88	5.35
	PM3	-8.740	-1.242	7.498	-2509.06	-2501.00	-2510.95	8.06	1.89	0.16	6.25	4.98
	AMI	-8.910	-1.150	7.76	-2759.38	-2751.23	-2761.27	8.15	1.89	0.16	6.25	5.02
	RMI	-8.839	-1.022	7.817	-2729.79	-2721.74	-2731.61	8.05	1.82	0.16	6.25	4.94
	MNDO	-8.944	-1.192	7.752	-2766.26	-2758.09	-2768.17	8.17	1.91	0.16	6.25	5.04

The energy of the highest occupy molecular orbital (E_{HOMO}) measures the tendency towards the donation of electron by a molecule [28]. Therefore, higher values of E_{HOMO} indicate better tendency towards the donation of electron, enhancing the adsorption of the inhibitor on mild steel and therefore better inhibition efficiency. From the results of the quantum chemical calculations, it evident that IG which is the best inhibitor has the highest value of E_{HOMO}. This indicates that IG would be better adsorbed on mild steel surface via electron donation compared to IS. On the other hand, the energy of the lowest occupied molecular orbital (E_{LUMO}) indicates the tendency towards the acceptance of electron. Therefore, the lower the value of E_{LUMO} the better is the expected inhibition efficiency. The

difference between E_{LUMO} and E_{HOMO} is the energy gap of the molecule (i.e $E_{L-H} = E_{LUMO} - E_{HOMO}$). This difference represents the softness or hardness of the molecule. Soft molecules are more reactive than hard molecules. From the calculated quantum chemical parameters, it is also evident that IG been the best inhibitor has the least values of E_{L-H} and E_{LUMO} for all the Hamiltonians. Therefore the frontier molecular orbital theory can be used to compare the inhibition potentials of IG and IS.

According to Eddy and Ita [29], DFT is based on the principle that the energy of a molecule can be determined from the electron density instead of a wave function. The DFT based on the Hohnenberg-Kohn theorems has been acknowledged as a powerful tool that can be used for the prediction of the sites for electrophilic and nucleophilic attacks [30].

In DFT, the ground state energy of an atom or a molecule can be expressed in terms of its electron density $\rho(r)$. Also two chemical reactivity indices, namely chemical potential (Υ) and global hardness are defined as the first and second derivative of $TE(\rho)$ with respect to the number of electrons, Thus,

$$\Upsilon = [\delta TE/\delta N]_v \quad (24)$$

$$\eta = (\delta^2 TE/\delta N^2)_{V(r)} = \tfrac{1}{2}(\delta\Upsilon/\delta N)_{V(r)} \quad (25)$$

where TE is the total energy, η is the global hardness and N is the number of electrons in the molecule. Using the finite difference approximation, the global hardness and softness were evaluated using the following equations [31]

$$\eta = [(E_{(N-1)} - E_{(N)}) - (E_{(N)} - E_{(N+!)})] \quad (26)$$

$$S = 1/[(E_{(N-1)} - E_{(N)}) - (E_{(N)} - E_{(N+!)})] \quad (27)$$

where $E_{(N-1)}$, $E_{(N)}$ and $E_{(N+1)}$ are the ground state energies of the molecule with N-1, N and N+1 electrons respectively. Also, the ionization energy (IE) and the electron affinity (EA) of the molecules were calculated using the ground state energies of the respective systems as follows [32],

$$IE = E_{(N-1)} - E_{(N)} \quad (28)$$

$$EA = E_{(N)} - E_{(N+!)} \quad (29)$$

The electro negativity (χ) of the inhibitor molecule was evaluated as $\chi = (IE+EA)/2$. Values of IE, EA, η, χ and S calculated from equations 26 to 29 are presented in Table 4. From the results obtained, IG been the best inhibitor had the higher value of IE, EA and χ while values of S and η for both IG and IS were comparable.

The sites for electrophilic and nucleophilic attacks on IG and IS were analysed using the Fukui function, which can be written as follows [33];

$$f^{+} = (\delta\rho(r)/\delta N)^{+}{}_{\upsilon} = q_{(N+1)} - q_{(N)} \quad (30)$$

$$f^{-} = (\delta\rho(r)/\delta N)^{-}{}_{\upsilon} = q_{(N)} - q_{(N-1)} \quad (31)$$

where f^{+} is the fukui function for electrophilic attack, f^{-} is the fukui function for nucleophilic attack, ρ, $q_{(N+1)}$, $q_{(N)}$ and $q_{(N-1)}$ are the density of electron and the Mulliken/Lowdin charge of the atom with N+1, N and N-1 electrons. Calculated values of f^{+} and f^{-} for IG and IS are presented in Table 5. Also, the local softness for electrophilic and nucleophilic attacks can be written as the product of the Fukui function and the global softness, S [34],

$$s^{+} = (f^{+})S \quad (32)$$

$$s^{-} = (f^{-})S \quad (33)$$

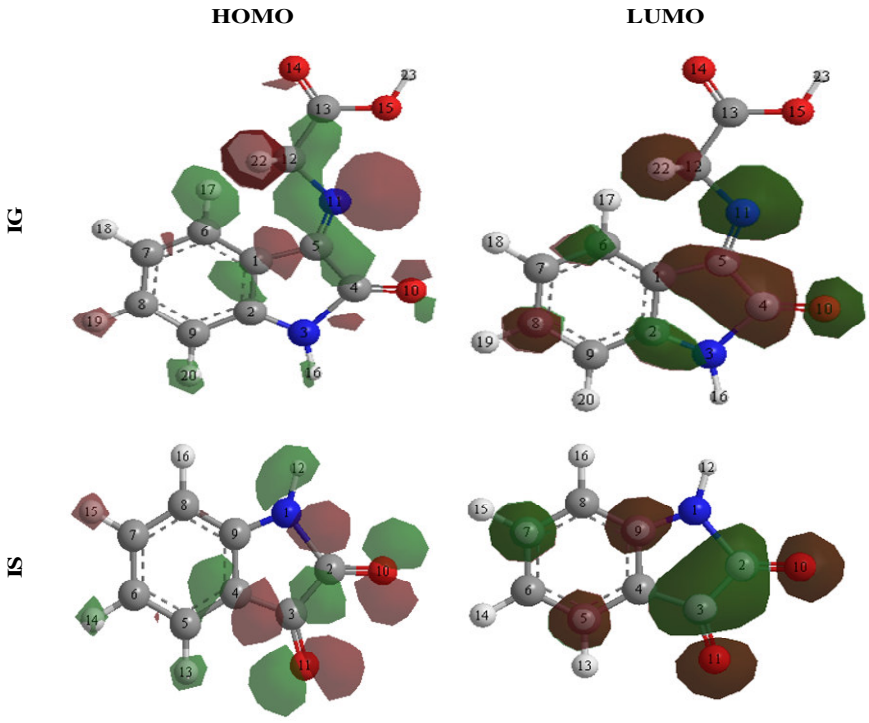

Figure 7. Molecular orbitals of IG and IS showing the HOMO and the LUMO.

Calculated values of s^{+} and s^{-} are also recorded in Table 5. Since there is similarity between the Fukui function and the frontier molecular orbitals, it is expected that the site for electrophilic attack is the site where the value of f^{+} is maximum while the site for nucleophilic attack is controlled by the values of f^{-}. From the results obtained, the sites for electrophilic attacks in IG and IS are in the pyrrole nitrogen (i.e N7 and N1 respectively) while the sites for nucleophilic attack are in the phenyl carbon (i.e C8 and C6 respectively).

Table 5. Huckel charge, Fukui and global softness indices calculated from Mulliken (Lowdin) charges for nucleophilic and electrophilic attacks on atoms in IG and IS

	Atom No	f^+ (|e|)	f^- (|e|)	S^+ (eV|e|)	S^- (eV|e|)	Huckel charge
IG	1 C	0.1062(0.0291)	-0.0251(-0.0293)	0.1698(0.0465)	-0.0401(-0.0468)	-0.1514
	2 C	0.0005(-0.0620)	0.0114(-0.0028)	0.0008(-0.0991)	0.0182(-0.0044)	-0.0212
	3 C	-0.0190(0.0174)	-0.0267(-0.0314)	-0.0304(0.0279)	-0.0427(-0.0503)	-0.1681
	4 C	0.1739(0.0707)	-0.0300(-0.0157)	0.2782(0.1131)	-0.0480(-0.0252)	-0.0756
	5 C	-0.4303(-0.0419)	0.0092(0.0089)	-0.6885(-0.0670)	0.0146(0.0142)	0.1717
	6 C	-0.1088(-0.0476)	0.0253(0.0229)	-0.1740(-0.0762)	0.0405(0.0366)	-0.1001
	7 N	0.6916(0.0818)	-0.0207(-0.0213)	1.1066(0.1309)	-0.0330(-0.0341)	0.2029
	8 C	-0.4109(-0.1417)	0.0465(0.0633)	-0.6574(-0.2268)	0.0744(0.1013)	0.4221
	9 C	-0.2224(-0.1099)	-0.0307(-0.0223)	-0.3559(-0.1758)	-0.0491(-0.0357)	0.1380
	10 O	-0.0255(-0.1559)	-0.0819(-0.0950)	-0.0408(-0.2494)	-0.1310(-0.1520)	-0.5747
	11 C	0.1686(0.0431)	-0.0002(-0.0044)	0.2697(0.0690)	-0.0004(-0.0070)	-0.0098
	12 N	0.0731(-0.1398)	0.0160(0.0112)	0.1169(-0.2237)	0.0257(0.0180)	-0.1776
	13 C	-0.3134(0.0142)	-0.0575(-0.0741)	-0.5014(0.0226)	-0.0921(-0.1185)	0.5751
	14 O	0.0965(-0.0118)	-0.4634(-0.5159)	0.1544(-0.0188)	-0.7414(-0.8255)	-0.6609
	15 O	0.2307(0.0560)	-0.1374(-0.1485)	0.3691(0.0897)	-0.2198(-0.2377)	-0.1514
IS	1 N	0.1010(0.0624)	-0.0535(-0.0445)	0.1616(0.0999)	-0.0713(-0.0856	0.1802
	2 C	-0.0759(-0.0469)	-0.0352(-0.0539)	-0.1214(-0.0751)	-0.0863(-0.0564)	0.4289
	3 C	-0.0016(-0.0270)	-0.0592(-0.0751)	-0.0025(-0.0431)	-0.1202(-0.0947)	0.3468
	4 C	-0.1039(-0.1049)	-0.0014(0.0197)	-0.1662(-0.1679)	0.0316(-0.0023)	-0.0923
	5 C	-0.1492(-0.1685)	-0.0078(0.0038)	-0.2388(-0.2695)	0.0061(-0.0124)	0.0045
	6 C	-0.0770(-0.0792)	0.0024(0.0193)	-0.1232(-0.1268)	0.0309(0.0039)	-0.1559
	7 C	0.0264(-0.0058)	-0.0274(-0.0624)	0.0423(-0.0094)	-0.0999(-0.0438)	0.0156
	8 C	-0.0480(-0.0911)	-0.0215(-0.0599)	-0.0768(-0.1458)	-0.0959(-0.0344)	-0.1667
	9 C	0.0051(-0.0002)	-0.0282(-0.0340)	0.0082(-0.0003)	-0.0544(-0.0451)	0.2002
	10 O	-0.1482(-0.1580)	-0.3168(-0.3909)	-0.2372(-0.2528)	-0.6255(-0.5068)	-0.4366
	11 O	-0.1848(-0.2018)	-0.1467(-0.1542)	-0.2957(-0.3228)	-0.2467(-0.2348)	-0.4862

In Fig. 7, the frontier molecular orbitals of IG and IS (green represent positive while maroon represent negative) are presented. It is significant to state that the HOMO corresponds to the nucleophilic Fukui function (f^-) while the LUMO correspond to the electrophilic Fukui function (f^+). Fig.7 reveals that there is an uneven and a high distribution of positive and negative charge around the pyrrole ring suggesting that electrophilic attack is likely within this region. On the other hand, the positive and negative lobes are scantily distributed around the phenyl ring, which indicate that this region is the expected site for nucleophilic attack.

In Tables 5, the Huckel charges on carbon and other electronegative elements in IG and IS are presented. From the calculated Huckel charges, it is evident that the highest positive charges in IG and IS are resident in the phenyl carbon (i.e C8 and C2 respectively) and in the pyrrole nitrogen (i.e N7 and N1 respectively). However, nitrogen is more electronegative than carbon therefore the prefer site

for electrophilic attack is in the pyrrole nitrogen. This assertion is consistent with the findings deduced from Fukui and global indices.

3.5. Mechanism of inhibition

The fact that the adsorption of IG and IS on mild steel surface proceeded via chemical adsorption indicate that the mechanism is consistent with the transferred of electron from the inhibitor's molecule to the empty orbital of Fe in mild steel. It is an established fact that the centre for the adsorption of an inhibitor on the surface of the metal is a hetero (such as N, O, or P). Having established that the centre for the adsorption of IG and IS on mild steel surface is in the pyrrole nitrogen, we hereby propose that the mechanism involves the protonation of the pyrrole nitrogen to form NH_3^+ by HCl solution. Therefore, the cationic form of the inhibitors immersed in the acidic medium can compete with hydrogen proton (H^+) for the electrons on the metallic surface. Since the size of the inhibitor's cation is much larger than that of hydrogen molecule (due to the presence of the amino structures in the inhibitors), after the release of H_2, the inhibitor returns to its neutral form with the electronegative group having a free electron pair that can facilitate its adsorption on mild steel surface. The adsorbed inhibitor can then protect the metal against further corrosion attack by blocking its active sites.

4. CONCLUSION

IG and IS are adsorption inhibitors for the corrosion of mild steel in HCl solution. The inhibition potential of IG is better than that of IS because the presence of methylenecarbamic acid group (=NCH_2CO_2H) offers better adsorption potentials than the =O group in IS. The mechanism of inhibition of mild steel corrosion by IG and IS involves chemisorption of the inhibitor (via the pyrrole nitrogen) on the metal surface. The adsorption of the inhibitors is spontaneous, exothermic and is characterized by increasing degree of orderliness.

References

1. A.K. Dubey, G. Singh, *Portugaliae Electrochimica Acta* 25(2007)249.
2. P.C. Okafor, S. Nesic , *Chem. Eng. Comm.* 194(2007) 141.
3. M.A. Quraishi, M.Z.A. Rafique, S. Khan, N. Saxena, *J. Appl. Electrochem.* 37 (2007) 1153.
4. G. Achary, H.P. Sachin, Y.A. Naik, T.V. Venkatesha, *Mater. Chem.& Phys.* 107(2008) 44.
5. S.A. Umoren, O. Ogbobe, I.E. Igwe, E.E. Ebenso, *Corros. Sci.* 68(2008) 4123.
6. M. Abdallah, *Corros. Sci,,* 46 (2004) 1981.
7. N.O. Eddy, P.A.P. Mamza, *Portugaliae Electrochimica. Acta* 27(2) (2009) 20.
8. N.O. Eddy, E.E. Ebenso, *Pigment and Resin Technology* 39(2) (2010) 77.
9. N.O. Eddy, E.E. Ebenso, *Int. Jour. Electrochem. Sci.* 5 (2010) 731.
10. P.C. Okafor, E.E. Ebenso, U.J. Ekpe, *Int. Jour. Electrochem. Sci.* 5 (2010) 978.
11. E.E. Ebenso, H. Alemu, S.A. Umoren, I.B. Obot, *Int. Jour. Electrochem. Sci.* 3 (2008) 1325.

12. K. Barouni, L. Bazzi, R. Salghi, M. Mihit, B. Hammouti, A. Albourine, S. El Issami, *Mater. Lett.* 62(2008)3325.
13. J. Fang, J. Li, *J. Mol. Struct. (Theochem)* 593(2002) 179.
14. N.O. Eddy, S.A. Odoemelam, *Pigment and Resin Technol.* 38(2) (2009)111.
15. E.E. Ebenso, U.J. Ekpe, B.I. Ita, O.E. Offiong, U.J. Ibok, *Mater. Chem.& Phys. 60* (1999) 79.
16. N.O. Eddy, S.A. Odoemelam, N. Ibiam, *J. Surface Sci. Technol*. 25 (3-4): (2009) 1.
17. J.P. Steward. MOPAC (2009). Steward Computational Chemistry, Version 9.069W. HTTP://OpenMOPAC.net
18. M.W. Schmidt, K.K. Baldridge, et al, Games version 12, *J. Comp. Chem*. (1993) 1347
19. N.O.Eddy, U.J. Ibok, E.E. Ebenso, *J. Appl. Electrochem.* 40 (2010) 445.
20. N.O.Eddy, U.J. Ibok, E.E. Ebenso, A. El Nemr, H. El Ashry, *J. Mol. Mod.* 15 (2009) 1085.
21. N.O.Eddy, E.E. Ebenso, *J. Mol. Mod.* 16(2010) 1291.
22. M.A. Quraishi, I. Ahmad, A.K. Singh, S.K. Shukla, *Mater. Chem. & Phys.*112 (2008) 1035.
23. K.N. Mohana, A.M. Badiea, *Corros. Sci.* 50 (2008) 2939.
24. S.A. Umoren, I.B. Obot, L.E. Akpabio, S.E. Etuk, *Pigment & Resin Technol.* 37(2) (2008): 98
25. S. Sternberg, V. Branzoi, *Electrochim. Acta* 29 (1984) 15.
26. E.A. Noor, *J. Appl. Electrochem.* 39 (2009) 1465.
27. S.T. Arab, A.M. Al-Turkustani, *Portugaliae Electrochimica Acta* 24(2006): 53.
28. H.E. El Ashry, A. El Nemr, S.A. Esawy, S. Ragab, *Electrochimica Acta* 51 (2006) 3957.
29. N.O.Eddy, B.I. Ita *Intern. J. Quant. Chem.* (2011) DOI: 10.1002/qua
30. P. Fuentealba, P. Perez, R, Contreras,*J. Chem. Phys.*13 (7)(2000) 2544.
31. N.O.Eddy *Mol. Simul.* 35(5) (2010) 354.
32. S.R. Stoyanov, S. Gusarov, S.M. Kuznick, A. Kovalenko, *J. Phys. Chem. C* 112: 6794.
33. B. Gomez, N.V. Likhanova, M.A. Dominguez, R.A. Martinez-Palou, A. Vela , J.L. Gazquez, *J. Phy. Chem. B.* 10(2006) 8928.
34. H. Wang, X. Wang, H. Wang, L. Wang, A. Liu, *J. Mol. Model.* 13(2007)147.